Crystal nucleation in a glass during relaxation well below T_g

Alexander S. Abyzov[a,b], Vladimir M. Fokin[b,c], Nikolay S. Yuritsyn[d], Marcio L. F. Nascimento[c], Jürn W. P. Schmelzer[e], Edgar D. Zanotto[b]

[a] National Science Center Kharkov Institute of Physics and Technology, 1, Akademicheskaya St., 61108 Kharkov, Ukraine
[b] Vitreous Materials Laboratory, Department of Materials Engineering, Federal University of São Carlos, UFSCar, Brazil
[c] Department of Chemical Engineering, Federal University of Bahia, Brazil
[d] Institute of Silicate Chemistry of Russian Academy of Sciences, nab. Makarova 2, 199034 St. Petersburg, Russia
[e] Institut für Physik der Universität Rostock, Albert-Einstein-Strasse 23-25, 18059 Rostock, Germany

Abstract

Until quite recently, in almost all papers on crystal nucleation in glass-forming substances it was assumed that nucleation proceeds in a completely relaxed supercooled liquid and hence at constant values of the critical parameters determining the nucleation rate for any given set of temperature, pressure, and composition. Here, we analyze the validity of this hypothesis for a model system by studying nucleation in a lithium silicate glass treated for very long times (up to 250 days) in deeply supercooled states, reaching 60 K below the laboratory glass transition temperature, T_g. At all temperatures in the considered range, $T<T_g$, we observed an enormous difference between the experimental number of nucleated crystals, $N(t)$, and its theoretically expected value computed by assuming the metastable state of the relaxing glass has been reached. Analyzing the origin of this discrepancy, we confirmed that the key parameters determining the nucleation rates *change with time* as a result of the glass relaxation process. Finally, we demonstrate that, for temperatures below 683 K, this particular glass almost fully crystallizes *prior to* reaching the ultimate steady-state nucleation regime (e.g., at 663 K, it would take 176 years for the glass to reach 99% crystallization, while 2,600 years would be needed for complete relaxation). This comprehensive study proves that structural relaxation strongly affects crystal nucleation in deeply supercooled states at temperatures well below T_g, hence this phenomenon has to be accounted for in any crystal nucleation model.

Keywords: Nucleation, crystal growth, glass, glass transition, phase transition theory

PACS numbers:

64.60.Bd General theory of phase transitions

64.60.Q Nucleation

64.70.Q Theory and modeling of the glass transition

70.kj Glasses

82.20.Rp Relaxation

1. Introduction

Crystallization is one of the most frequently used keywords in glass science and technology papers having appeared approximately 130,000 times in glass-related studies at the Scopus database (searching with glass* and crystal*). Such impressive statistics highlights the vital importance of crystallization for glass formation and development of novel glass-ceramics.

To analyze crystal nucleation experiments, as well as to predict nucleation rates, the Classical Nucleation Theory (CNT), developed in the 1920-40s[1-7], has been frequently employed. For temperatures above the conventional laboratory glass transition temperature, T_g, the CNT allows a reasonably correct treatment of the nucleation kinetics. However, already at the early 1980s, some researchers [8-10] noticed that, at temperatures near and below T_g, the crystal nucleation rates measured in silicate and metallic glasses were much *lower* than the theoretically expected values obtained by extrapolation of the curves calculated by the CNT based on nucleation data above T_g. This discrepancy drastically increases with decreasing temperature and has been denoted as the "breakdown of CNT" or "CNT failure".

Different ideas have been proposed, with limited success, to explain this discrepancy between the experimental nucleation rates and their theoretical predictions for $T < T_g$ [11-14]. In these works, changes in the glass that could affect the nucleation kinetics were considered. In contrast, analysis of nucleation data was limited to the nucleation rate interpreted as a steady-state one. However, the theoretical analysis of nucleation experiments should be wider than just describing the steady-state nucleation rate and its temperature dependence. It should also include a description of the *entire* dependence of the number of crystals, $N(t)$, on nucleation time, including the early stages. Ignoring the early stage of transformation leads to an erroneous interpretation of the time dependence of the nucleation rate as an establishment of its steady state regime described in CNT.

Another approach to solving this problem of deviation of experimental results and theoretical predictions of nucleation kinetics was recently proposed and developed in refs.[15-19]. It consists in the following: in almost all papers on nucleation in glass-forming substances it was assumed that nucleation proceeds in a completely relaxed supercooled liquid, and hence at constant sets of the key parameters determining the nucleation rate (the thermodynamic driving force, the surface energy of the crystalline clusters, and the effective diffusion coefficient governing the aggregation processes). In other words, almost all previous studies dealing with crystallization kinetics, e.g., refs.[8-Error! Bookmark not defined.], have assumed that relaxation *precedes* crystal nucleation and growth processes.

Structural relaxation and crystallization have been discussed in recent years for different materials, such as chalcogenide glasses[20], polymers[21,22], and metallic glasses[23]. In these four

works, it was concluded that relaxation is completed *before* crystallization becomes significant. However, we emphasize that in these papers the crystallization process was detected only at relatively advanced stages, that is, significantly after the beginning of nucleation. One should also recall that at temperatures below the glass transition range, despite the significant number of nucleated crystals, very long times are needed to detect them they due to their very low growth rate. Thus, we suppose that the nucleation process began much earlier than the crystallization signs detected in these four works.

Yet on this topic, it is worth mentioning recent research[24,25] in which molecular dynamics simulations revealed an increase in the free energy of nucleation and in the critical nucleus size as the supercooling increased. According to our model, this unusual behavior is likely due to the insufficient time for complete relaxation of the supercooled liquid (SCL), which leads to lower nucleation rates compared to their steady-state values.

As we showed previously for some silicate glasses in[15-19], and for lithium disilicate in the present work, at temperatures below T_g crystal nucleation starts in a glass whose relaxing structure has not yet reached the metastable equilibrium state corresponding to the temperature and pressure under study. *This feature is the main origin of the discrepancy* between the experimental and theoretical (corresponding to the completely relaxed glass that reached the SCL state) values of steady-state nucleation rates. By properly accounting for the effect of the changes of the thermodynamic and kinetic parameters of the relaxing liquid on crystal nucleation and growth, a correct description of nucleation can be achieved in terms of the CNT, as recently demonstrated in refs.[15-19]. Consequently, CNT does *not* breakdown at T_g; however, it has to be employed in an appropriate way accounting for the current state of the relaxing glass during nucleation and the change of this state over time caused by relaxation.

In this paper, we advance our previous works on low-temperature nucleation by extending the study to much deeper supercoolings, reaching temperatures down to $\boldsymbol{T = T_g - 60\ \mathrm{K}}$. In this case, we obtained and analyzed a new set of nucleation rate data for a lithium disilicate glass (used here as a model system) treated for extremely long times, which reached up to 250 days at the lowest temperature. We paid special attention to the temperature dependences of the characteristic times of structural relaxation and the times necessary for significant crystallization. Also, for a set of temperatures below T_g, several linear sections were distinguished on the plots of number of crystallites, $N(t)$, as a function of time. We interpret this behavior as a consequence of the stepwise nature of structural relaxation below T_g, which we had been previously demonstrated only for a single temperature.

2. Materials and Methods

In this work, we used samples of the same $32.55Li_2O{\cdot}67.45SiO_2$ mol% (by analysis) glass used earlier. Its composition is quite close to that of stoichiometric lithium disilicate ($33.33Li_2O{\cdot}66.67SiO_2$). The glass preparation is described in detail in ref.[15].

To achieve visible crystal sizes under an optical microscope, following the Tammann "development" method[26], a second heat treatment at $T_d > T$ was performed for crystal growth after nucleation at a temperature $T < T_d$. The crystal number densities, N [crystals/mm^3], were calculated via the number of crystal traces on polished cross-sections of the treated samples using stereological methods and reflected light microscopy (see, e.g., ref.[27]). When N was very small (typical case for short nucleation times or very low nucleation temperature), plane-parallel thin plates with polished sides were prepared for direct estimation of the crystal number in a given volume by transmitted light. These two methods were compared for some samples and yielded the same values of N. The average error was determined from statistics of randomly probed areas on sample cross sections, or of certain volumes viewed on a thin transparent plate.

3. Theoretical description

As we have shown in recent works[15-19] and briefly reviewed in the Introduction section, the time dependence, $N(t)$, of the number of supercritical clusters cannot be described by the CNT at temperatures below T_g using a constant set of parameters (diffusivity, driving force, and interfacial energy) determining the nucleation rate. In this temperature range, these parameters depend on the current state of the liquid undergoing the relaxation process. Therefore, to account for their temporal changes due to structural relaxation, we introduced into the CNT equations a *structural order parameter*, $\zeta(t)$, which reflects the relaxation of supercooled liquid toward the metastable equilibrium state.

Below we present the main expressions used here to theoretically describe the experimental dependences, $N(t)$. The following equation for the steady-state nucleation rate, I_{st}, in *a relaxing* glass or liquid, was derived in our previous works[17,18,28]:

$$I_{st}(T,t) = \frac{1}{d_0^3}\sqrt{\frac{\sigma_{eq}(T)\zeta(t)}{k_B T}}\frac{2D(T,t)}{d_0}\exp\left(-\frac{W_{c,eq}(T)\zeta(t)}{k_B T}\right), \quad (1)$$

$$D(T,t) = D_0\exp\left(-\frac{E_U\zeta(t)}{k_B T}\right), \quad (2)$$

where k_B is the Boltzmann constant, T is the absolute temperature, $d_0 = 4.8 \cdot 10^{-10}$m is the effective size of the structural units estimated as $d_0 = (V_M/N_A)^{1/3}$ via the crystal molar volume, V_M, and the Avogadro number, N_A. $W_{c,eq}$ is the work of formation of a critical sized nucleus, R_{cr}:

$$W_{c,eq} = \frac{16}{3}\pi \frac{\sigma_{\mathrm{eq}}^3}{\Delta G_{\mathrm{V,eq}}^2}, \tag{3}$$

$$R_{cr} = 2\sigma_{eq}/\Delta G_{\mathrm{V,eq}}, \tag{4}$$

where σ_{eq} is the surface energy of the critical nucleus/ supercooled liquid interface, which we estimated using the Tolman equation:

$$\sigma_{\mathrm{eq}}(T) = \frac{\sigma_0}{1 + \frac{2\delta}{R_{cr}(T)}}. \tag{5}$$

The surface tension of a planar interface, $\sigma_0 = 0.1903\ \mathrm{J/m^2}$, and the Tolman parameter, $\delta = 2.92 \cdot 10^{-11}$m, in Eq. (5) were obtained from a fitting procedure to best describe the experimental steady-state nucleation rates, I_{st}, at relatively high temperatures $T \geq 713$ K ($T_g \approx 726$ K).

The effective diffusion coefficient, D, in Eqs. (1) and (2) for the completely relaxed liquid was estimated from the experimental crystal growth rate data ($D|_{t\to\infty} = D_U$), assuming the screw dislocation growth model[29]:

$$U = D_U \frac{T_m - T}{8\pi d_0 T_m}\left[1 - \exp\left(-\frac{|\Delta G_{\mathrm{V,eq}}|\, d_0^3}{k_B T}\right)\right], \tag{6}$$

where T_m is the melting point and $\Delta G_{\mathrm{V,eq}}$ is the change of the bulk contributions to the Gibbs free energy per unit volume of the crystal phase[30]:

$$\Delta G_{\mathrm{V,eq}}(T) = 8.40245024 \cdot 10^8 - 540266 \cdot T - 78.5116 \cdot T^2, \tag{7}$$

with T in Kelvin and $\Delta G_{\mathrm{V,eq}}$ in $\mathrm{J/m^3}$.

In Eq.(2), D_0 and E_U were chosen to best fit D_U shown in Fig. 1: D_0=1.882 $\cdot 10^4$ m^2/s, $E_U = 5.374 \cdot 10^{-19}$ J for $T > T_{sd}$=764K, and D_0=1.2 $\cdot 10^{-10}$ m^2/s , $E_U = 6.9035\ 10^{-20}/(1 - T_0/T)$ J for $T \leq T_{sd}$ with $T_0 = 490.17$K.

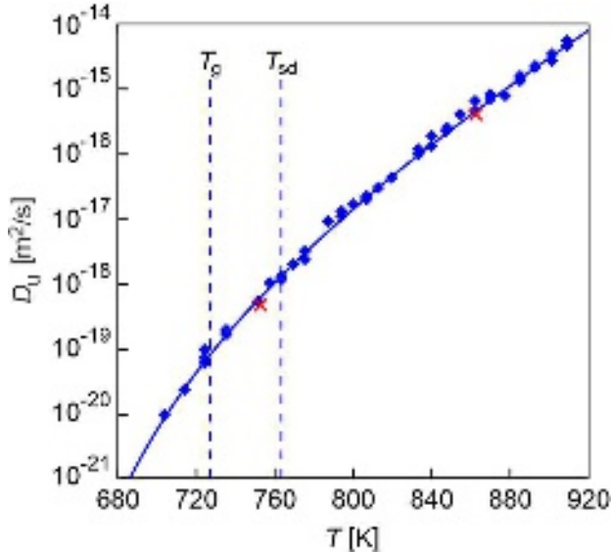

FIG. 1. Diffusion coefficient, D_U, determining crystal growth velocities *vs*. temperature in lithium disilicate glass. The red crosses and diamonds represent the data calculated from the experimental growth velocities in the glass used in the present paper and taken from[31], respectively. The solid blue line was plotted by Eq. (2) with $\zeta = 1$.

In the model employed here, a value of the structural order parameter $\zeta(t) = 1$ corresponds to complete relaxation, deviations from equilibrium of the liquid are described by $\zeta(t) > 1$. The time dependence of the structural order parameter was approximated by the Kohlrausch stretched exponent law:

$$\zeta(t) = 1 + \zeta_0 \cdot \exp\left[-\left(\frac{t}{\tau_{sr}}\right)^{\beta}\right], \tag{8}$$

where ζ_0, τ_{sr} and β are fitting parameters for the best agreement of the calculated $N(t)$ dependence:

$$N(t) = \int_0^t I_{st}(t')dt' \tag{9}$$

with the experimentally measured $N(t)$ values at each temperature.

3. Results and discussion

3.1 Change of the nucleation rates with time and its theoretical description

Figures 2 - 6 show the number of crystals per unit volume, *N*, versus nucleation time, *t*, at $T = 663$ K, 683 K, 693 K, 713 K and 723 K ($T_g \approx 726$ K) respectively, obtained by Tammann's "development" treatment at $T_d = 863$ K after nucleation.

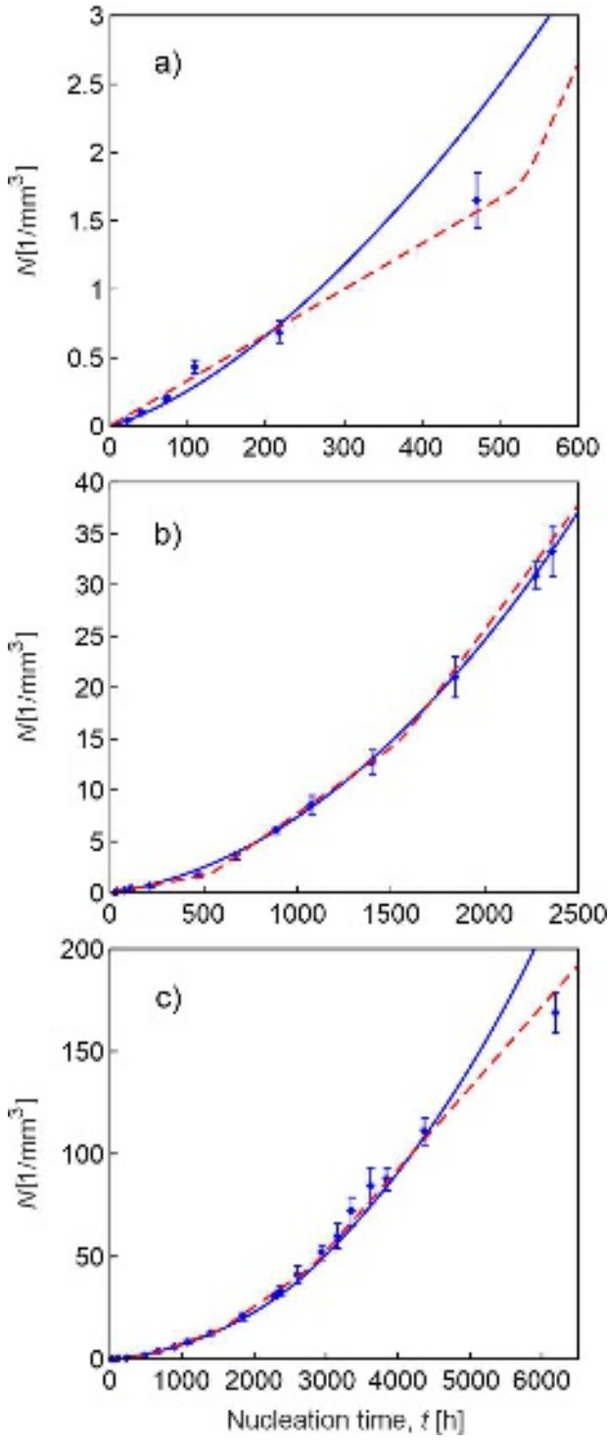

FIG. 2. Crystal number density *vs*. nucleation time at 663 K. Rhombuses are the experimental data. The solid blue line was plotted by Eq. (9) with $\zeta(t)$ approximated by the Kohlrausch stretched exponent equation (Eq. (8)). The dashed red line corresponds to the stepwise evolution of the structural order parameter that allows the best description of the experimental data. Indexes correspond to different nucleation times considered in this analysis: short (a); average (b) and long (c) observations.

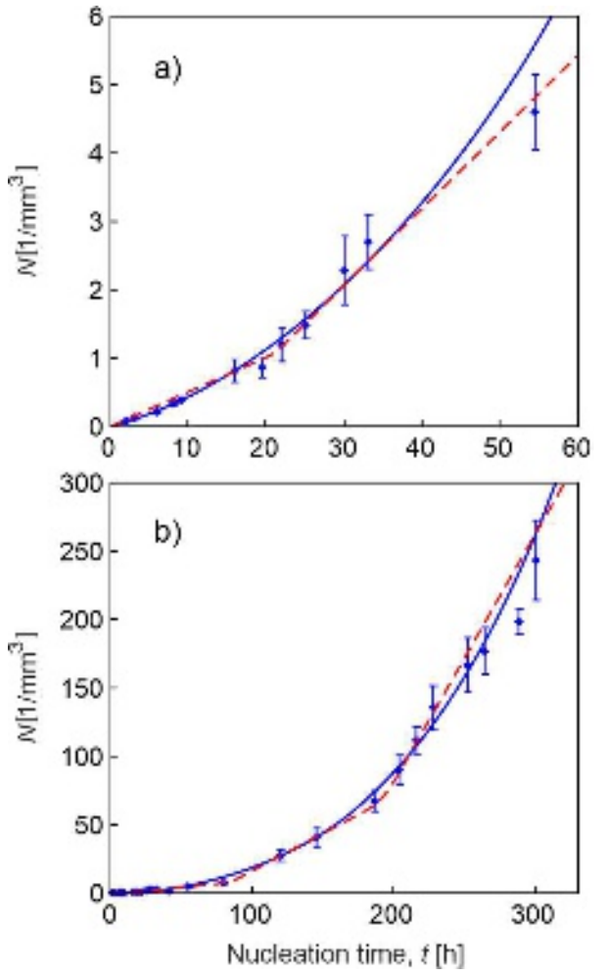

FIG. 3. Crystal number density *vs*. nucleation time at 683 K. Rhombuses are the experimental data. The solid blue line was plotted by Eq. (9) with $\zeta(t)$ approximated by the Kohlrausch stretched exponent equation (Eq. (8)). The dashed red line corresponds to the stepwise evolution of the structural order parameter that allows the best description of the experimental data. Indexes correspond to different nucleation times considered in this analysis: short (a); average (b) observations.

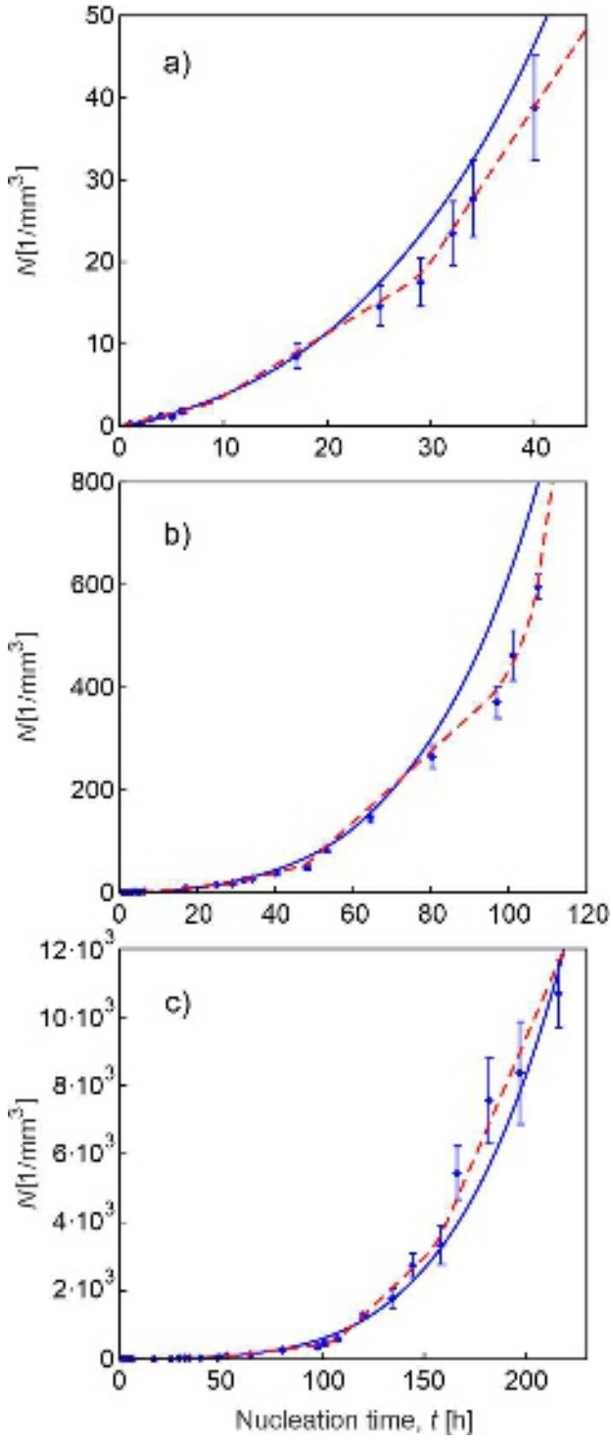

FIG. 4. Crystal number density *vs*. nucleation time at 693 K. Rhombuses are the experimental data. The solid blue line was plotted by Eq. (9) with $\zeta(t)$ approximated by the Kohlrausch stretched exponent equation (Eq. (8)). The dashed red line corresponds to the stepwise evolution of the structural order parameter that allows the best description of the experimental data. Indexes correspond to different nucleation times considered in this analysis: short (a); average (b) and long (c) observations.

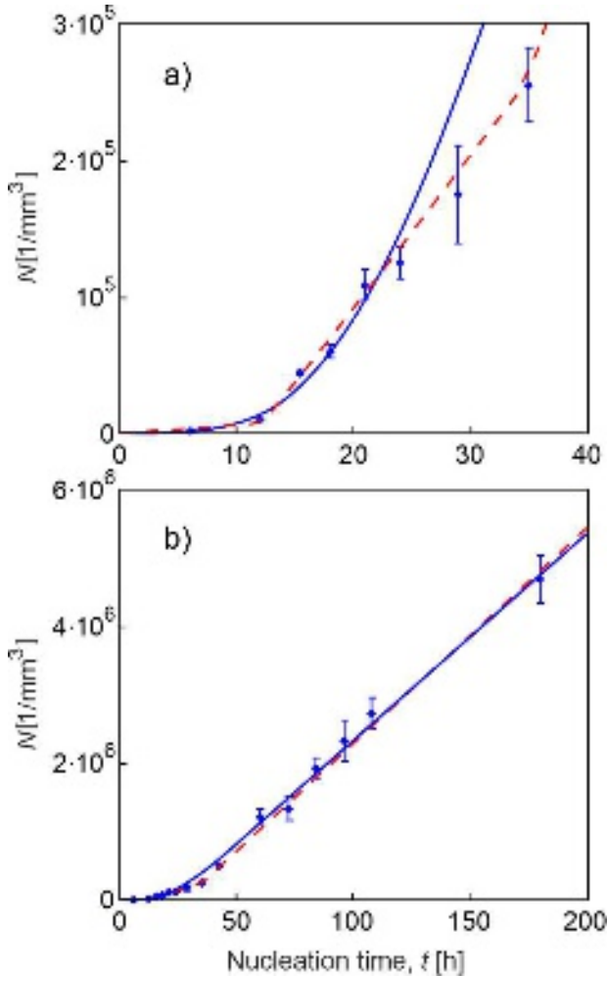

FIG. 5. Crystal number density *vs*. nucleation time at 713 K. Rhombuses are the experimental data. The solid blue line was plotted by Eq. (9) with $\zeta(t)$ approximated by the Kohlrausch stretched exponent equation (Eq. (8)). The dashed red line corresponds to the stepwise evolution of the structural order parameter that allows the best description of the experimental data. Indexes correspond to different nucleation times considered in this analysis: short (a); average (b) observations.

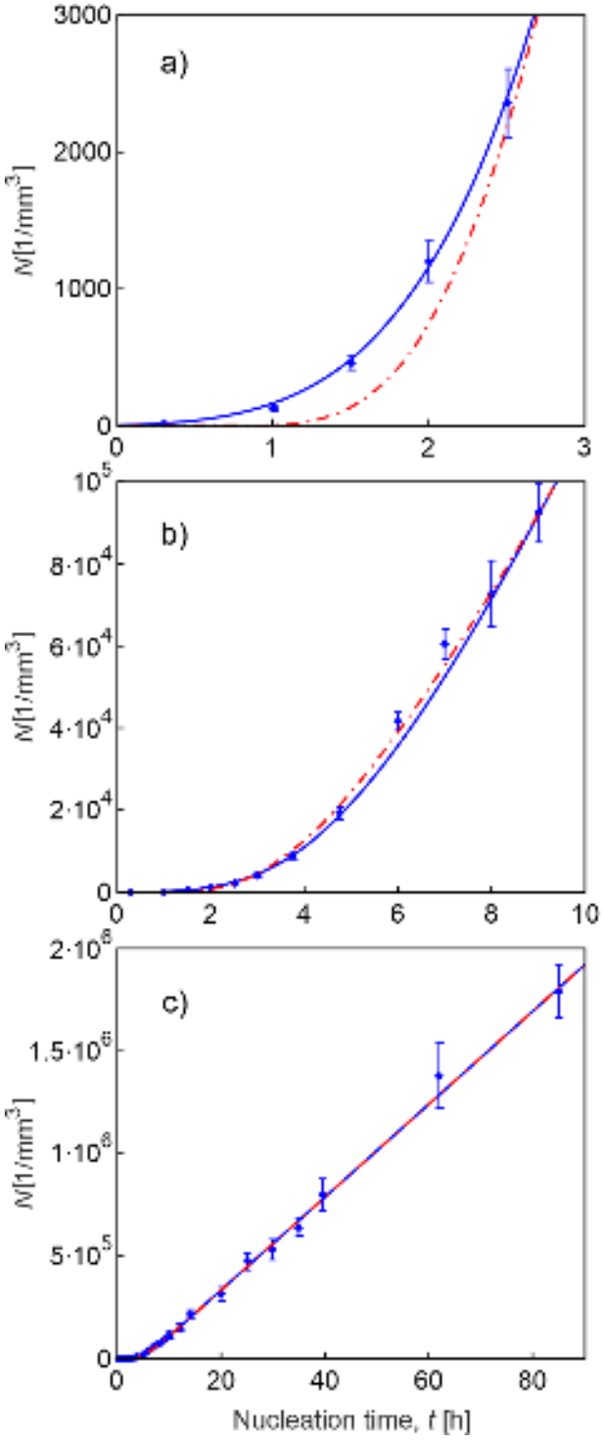

FIG. 6. Crystal number density *vs*. nucleation time at 723 K. Rhombuses are the experimental data. The solid blue line was plotted by Eq. (9) with $\zeta(t)$ approximated by the Kohlrausch stretched exponent equation (Eq. (8)). The dashed-dotted red line corresponds to the Collins-Kashchiev equation (Eq. (10)) with $I_{st} = 6.3 \cdot 10^9 \mathrm{m}^{-3}\mathrm{s}^{-1}$ determined by Eq. (1) at $t \to \infty$ and $\tau_{CK} = 3.2\mathrm{h}$ used as a fit parameter to describe the linear part of the experimental $N(t)$ − dependence. Indexes correspond to different nucleation times considered in this analysis: short (a); average (b) and long (c) observations.

As we have shown in recent papers[Error! Bookmark not defined.,Error! Bookmark not defined.,15] and discussed in the Introduction section, at temperatures below the glass transition interval, it is

impossible to adequately describe the experimental dependence of $N(t)$ using a constant set of parameters determining the nucleation rates. The dashed-dotted red line in Fig. 6 illustrates this statement. It was plotted by the Collins-Kashchiev equation[5,32]:

$$N_{CK}(t) = I_{st}\tau\left[\frac{t}{\tau} - \frac{\pi^2}{6} - 2\sum_{m=1}^{\infty}\frac{(-1)^m}{m^2}\exp\left(-m^2\frac{t}{\tau}\right)\right], \qquad (10)$$

with $I_{st} = 6.3 \cdot 10^9 \mathrm{m}^{-3}\mathrm{s}^{-1}$ determined by Eq. (1) at $t \to \infty$ and $\tau = 3.2\mathrm{h}$ used as a fit parameter to describe *only* the linear part of experimental $N(t)$ dependence. At short times, the $N(t)$ dependence passes significantly below the experimental points (Fig. 6a). This discrepancy is more visible in Fig. 7, which shows the N_{CK}/N ratio *vs*. nucleation time.

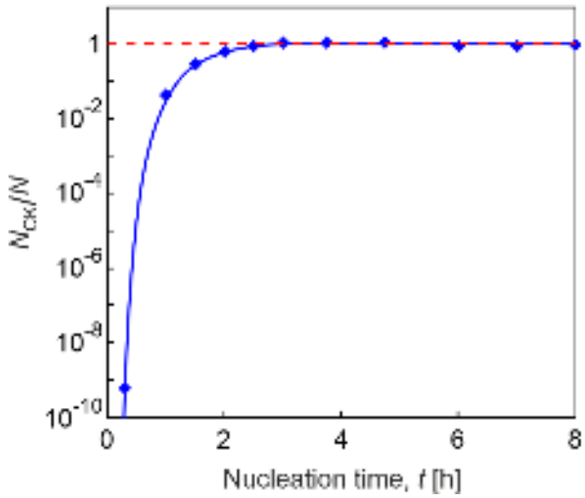

FIG. 7. N_{CK}/N ratio *vs*. nucleation time at 723 K. Points denote the ratio of experimental values of *N* to those estimated by Eq. (10). The solid blue line was obtained as the ratio of *N* estimated by of Eqs. (10) and (9). The dashed red line corresponds to the case when *N* is equal to N_{CK}.

Based on this result and refs.[15,17,18], we conclude that the main parameters determining the nucleation rate *change with time* because of the structural relaxation of the glass. This result shows once more the importance of the initial part of the $N(t)$ dependence for a correct description of the nucleation process at low temperatures, which cannot be neglected.

The solid lines in Figs. 2-6 were calculated by Eq. (9) considering the structural relaxation with parameters ζ_0, τ_{sr}, β of the Kohlrausch stretched exponent, which are shown in Figs. 8a, b, c, respectively, as a function of temperature.

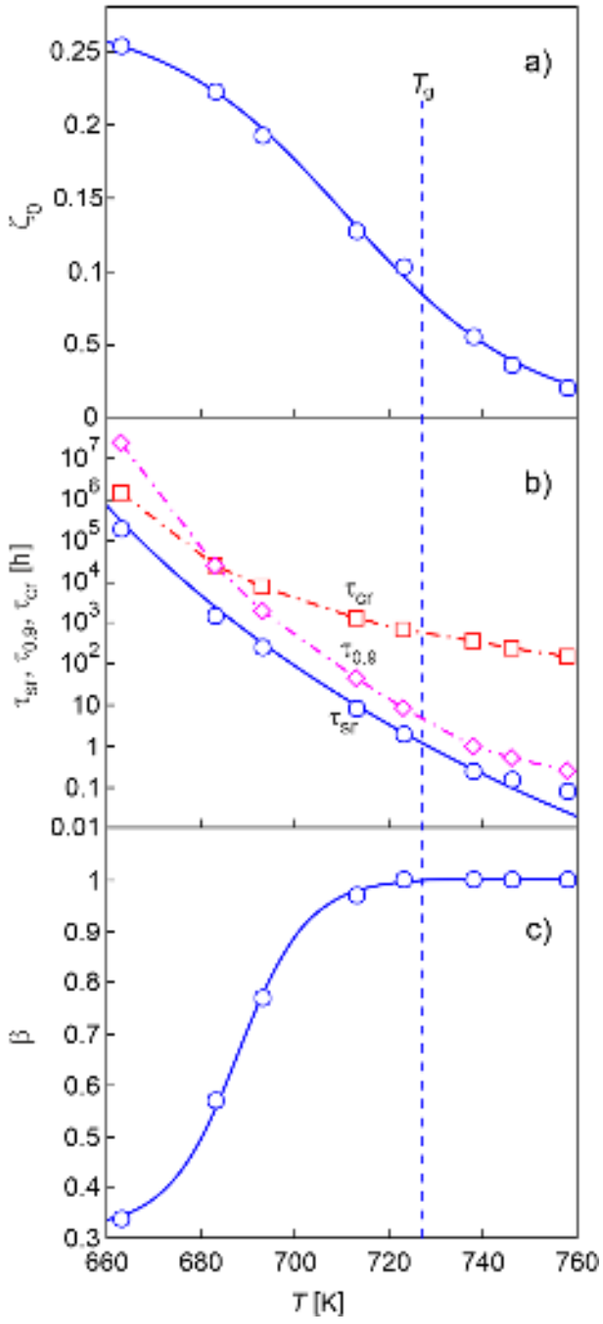

FIG. 8. Temperature dependences of the Kohlrausch stretched exponential parameters ζ_0, τ_{sr}, β (a, b, c, respectively), as a function of temperature parameters; the times $\tau_{0.9}$ and τ_{cr} needed to achieve $0.9 \cdot I_{st}(T)$ and the volume fraction crystallized, $\alpha = 0.99$, respectively. The solid blue lines are plotted by Eqs. (11), (12) and (13), respectively. The dash-dotted lines are only a guide to the eyes.

The temperature dependences of $\zeta_0(T)$, $\tau_{sr}(T)$, and $\beta(T)$ can be fitted with the following formulas:

$$\zeta_0(T) = 0.138\left[1 - \tanh\left(\frac{T-711}{39}\right)\right], \tag{11}$$

$$\tau_{sr}(T) = \frac{d_0^3}{2k_B T}\eta(T), \tag{12}$$

$$\beta(T) = 1 - 0.34\left[1 - \tanh\left(\frac{T-688}{15}\right)\right], \quad (13)$$

with T in Kelvin.

The viscosity in this relatively narrow temperature range is well described by the VFT equation:

$$\eta(T) = \eta_0 \exp\left(\frac{E_\eta}{k_B(T-T_0)}\right), \quad (14)$$

where $\eta_0 = 2.178$ Pa · s, $E_\eta = 1.091 \cdot 10^{-11}$J, and $T_0 = 490.17$ K[31].

These parameters give the best agreement between the calculated $N(t)$ dependences and the experimental data. It should be noted that the calculated $N(t)$ dependences finally reach a slope corresponding to the ultimate steady-state nucleation rate, $I_{st}(T)$, at any given temperature, including the temperatures (e.g., 663 and 683 K) at which this state *cannot be achieved* by actual experiments. The times required to complete relaxation are far too long to be experimentally accessible, and are longer than the time needed for significant crystallization.

It is noteworthy that the temperature dependence of τ_{sr} obtained from the analysis of the nucleation data (circles in Fig. 8b) is well described by Eq. (12). This allows us to assume that the structural relaxation resulting in a change (increase) in the nucleation rate is governed by the same or similar mechanisms as viscous flow. At the same time, as clearly shown in ref.[17], viscosity cannot be used to estimate the nucleation rates, and hence to describe the N *vs*. t dependence. Thus, viscosity influences the nucleation kinetics through its effect on structural relaxation. Despite the fact that both processes have similar temperature dependences, as we have shown in previous papers[15,17], the nucleation process to achieve the steady-state regime takes *much longer* than the classical alpha relaxation, which is largely governed by viscosity.

3.2 The effect of overall crystallization

Another interesting consequence follows from the crossover shown in Fig. 8b of the temperature dependences of the nucleation time, $\tau_{0.9}$, required to reach 90% of the ultimate steady-state nucleation rate and the crystallization time, τ_{cr}, needed to reach the crystalline volume fraction $\alpha = 0.99$, which can be calculated using the JMAK equation[5,6]:

$$\alpha(t) = 1 - \exp\left(-\int_0^t I\,(T,t')v(t-t')dt'\right), \quad (15)$$

$$v(t) = \frac{4\pi}{3}\left(\int_0^t U(t')dt'\right)^3, \quad (16)$$

where the nucleation rate, $I(T,t)$, is determined by Eq. (1) and the growth velocity is given by

$$U(T,t) = \frac{T_m - T}{8\pi d_0 T_m} D(T,t), \qquad (17)$$

with D estimated by Eq. (2).

Calculations with Eq. (15) indicated that, at temperatures *below* 683 K, the glass *crystallizes completely* (99%) before the nucleation rate reaches a steady-state value, since $\tau_{0.9}(T) > \tau_{cr}(T)$. Since, according to our model, the ultimate steady-state nucleation rate at a given temperature value, $I_{st}(T)$, can be achieved only in a completely relaxed glass, the latter cannot reach its metastable equilibrium state at $T < 683$ K. We obtained a similar result for a barium silicate glass[18]. Thus, the existence of a crossover temperature of $\tau_{0.9}(T)$ and $\tau_{cr}(T)$ indicates that the choice of a proper annealing temperature is quite important for the problem considered in refs.[20-23].

The two previously discussed processes – structural relaxation leading to a change in the nucleation rate and the overall crystallization – are illustrated in Fig. 9. The solid circles show the experimental values of the nucleation rates that have been reached at the times indicated. As previously mentioned, the nucleation kinetics for temperatures above 713 K could be described in the framework of the CNT as the ultimate steady-state nucleation rates, because the nucleation experiments at these temperatures were performed for larger times as compared to the time of structural relaxation. However, for temperatures below 713 K (e.g., 693, 683 and 663 K), the nucleation rates reached values in the orders of magnitude lower than those theoretically expected (hollow circles) despite the long and very long (up to 8.5 months) experimental times – in agreement with results shown in Figures 2 to 4. To achieve the theoretically expected steady-state nucleation rates, the times of the nucleation experiments must be significantly extended – denoted near the hollow circles. However, as previously shown for temperatures below 683 K, the ultimate steady-state nucleation regime cannot be achieved because of crystallization. Therefore, the change in the steady-state nucleation rate, as follows from the CNT, at temperatures below 683 K is shown by the dashed red line. The solid line for temperatures below 683 K corresponds to the maximum values of the nucleation rate that can be reached before complete crystallization.

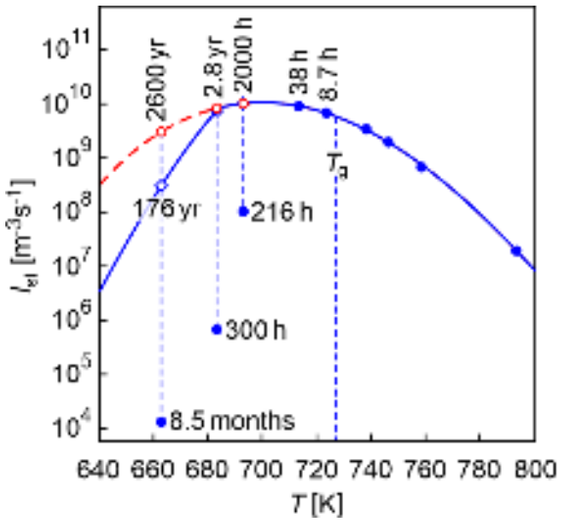

FIG. 9. Nucleation rates as a function of temperature. The dashed red line shows the theoretically expected nucleation rates, and the times $\tau_{0.9}$ are denoted above the hollow circles. The solid blue line corresponds to the maximum nucleation rates that can be reached before significant crystallization, whereas the times τ_{cr} are denoted close to the symbols. The solid circles show the experimentally measured nucleation rates that have been reached by the treatment times indicated.

It should be noted that to describe the $N(t)$ dependences we used Eq. (1) for the steady-state nucleation rate, which is only valid for the established steady-state nucleation regime, as described in the CNT. This was done for the following reason. As we established in ref.[Error! Bookmark not defined.] and show here in Fig. 10, the characteristic relaxation time, τ_{sr}, is in this temperature range much larger than the classical nucleation time-lag, τ_{ns}[32]:

$$\tau_{ns}(T,t) = \frac{16}{3}\frac{\sigma k_B T}{d_0^2 \Delta G_V^2 D(T,t)} \quad , \tag{17}$$

where $D(T,t)$ is estimated by Eq. (2).

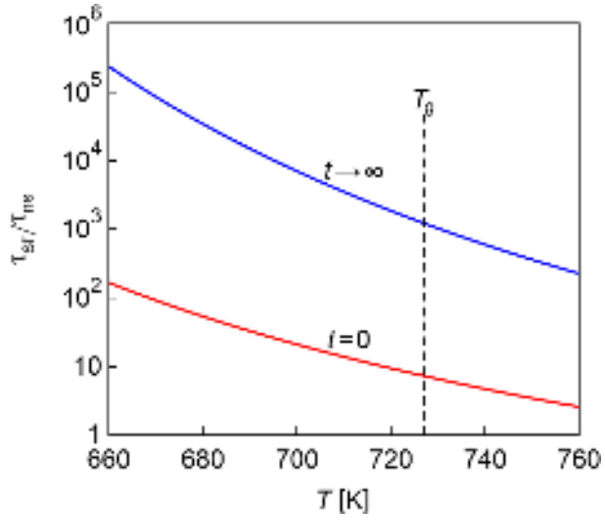

FIG. 10. The τ_{sr}/τ_{ns} time ratio as a function of temperature at the very beginning of the nucleation process ($t = 0$) and at an advanced stage ($t \to \infty$).

As follows from Fig. 10, during the nucleation process ($0 < t < \infty$), the inequality $\tau_{sr} \gg \tau_{ns}$ is valid up to temperatures above T_g. This means that, at each moment of time, the nucleation rate will be close to its steady-state value corresponding to the current state of the supercooled liquid.

3.3 Stepwise relaxation and nucleation

One of the most intriguing features of low-temperature nucleation is the stepwise increase in the nucleation rate, which we interpret as resulting from stepwise relaxation. As we have shown in ref.[15] for lithium disilicate glass at 703 K and in this work for a new set of temperatures: 713, 693, 683 and 663 K (Figs. 2-5), successive linear segments with increasing durations and slopes can be distinguished on the $N(t)$ dependences. These linear sections provide evidence for the unusual behavior of the "temporary" steady-state nucleation rates, which correspond to different states of the material (relaxing glass) in distinct time intervals.

The last linear part of the $N(t)$ dependence must correspond to the ultimate steady-state nucleation rate, which can only be achieved in a completely relaxed glass (that becomes a SCL). However, as previously discussed, below a certain temperature, the equilibrium state of the liquid cannot be reached because of the crystallization of the glass.

To take stepwise relaxation into account for a better description of the $N(t)$ dependences (see dashed lines in Figs. 2-5), we introduced a stepwise change of the structural parameter $\zeta(t)$ – an example is shown in Fig. 11. For 713 K, where the last step corresponds to $\zeta = 1$, that is, a completely relaxed SCL was achieved (Fig. 11a, see also Figs. 5b and 9). However, at a lower temperature, 683 K, the experimental time of 300 h is much shorter than the 2.8 years required for complete relaxation of the glass and achievement of the ultimate steady-state nucleation rate.

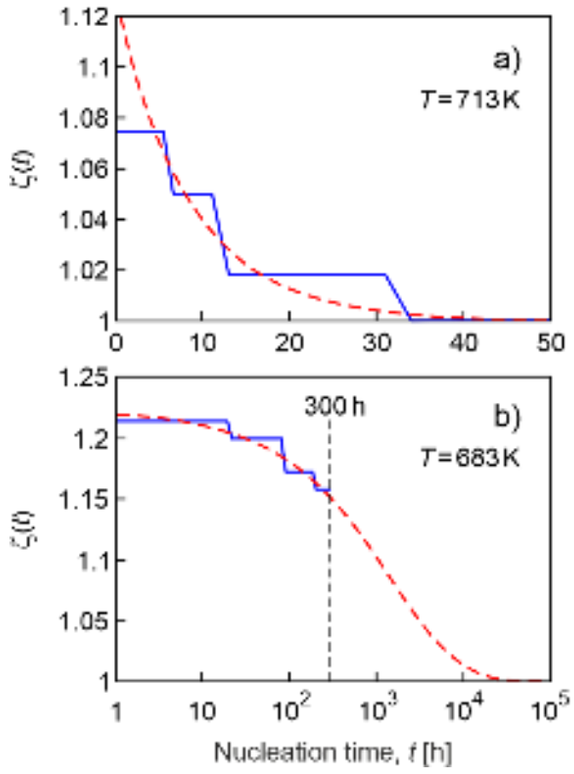

Fig. 11. Approximation by the Kohlrausch stretched exponent law (dashed red line) and stepwise evolution of the structural order parameter, ζ (solid blue line), at 713 K (a) and 683 K (b). The experimental time of 300 h is shown by the dashed black line.

Experimental evidence of stepwise structural relaxation is still quite rare (see also our previous studies[15-19]). As far as we know, this type of relaxation had already been observed in metal alloys[33], polymers[34], and chalcogenide glasses[20]. In fact, Gallino *et al.*[33] reported on multiple decays in the enthalpy change during aging of a bulk metallic glass with annealing treatments up to 50 K below T_g. And Cangialosi *et al.*[34] observed aging times up to one year from specific heat measurements. This interesting behavior of supercooled glass-forming liquids requires additional experimental study and deeper analyses.

6. Summary and Conclusions

For several reasons, understanding the crystal nucleation behavior at temperatures close to and below the glass transition is both relevant and fascinating. First, deep supercoolings are necessary to achieve a significant nucleation rate. Second, the exponential deceleration of all kinetic processes with decreasing temperature enables detailed studies of the nucleation kinetics starting from the very beginning, which is impractical at somewhat higher temperatures due to faster nucleation and crystal growth rates. This possibility allowed us to detect earlier and in the present work, for temperatures below T_g, an enormous difference between the experimental

number of nucleated crystals and the theoretically expected number obtained by assuming a constant state of the material. Based on these experimental facts, we conclude that the thermodynamic and kinetic parameters determining the nucleation rates change with time due to glass relaxation.

Only recently, the lack of data for the early stages of the dependences or their incorrect analysis has prevented researchers from understanding the reported discrepancy between experiments and calculations below T_g. Therefore, experimental nucleation induction periods have been erroneously interpreted as a consequence of the establishment of the stationary regime of nucleation described by the CNT.

In this work, by extending the study temperature range to 60 degrees below Tg and the nucleation times up to 250 days, we obtained the temperature dependence of the Kohlrausch stretched exponent parameters, which described the structural order parameter rather well. We found an agreement of the *temperature dependence* of the relaxation time, determined from the nucleation kinetics with the relaxation time estimated using viscosity (the classical α-relaxation). Despite these similar temperature dependences, which corroborate our previous papers on different materials, achieving the steady-state nucleation regime takes *much longer* than the classical α-relaxation, as measured, e.g., by density or refractive index variations.

Also, in analyzing the kinetics of overall crystallization by considering the effect of structural relaxation, we showed that, at temperatures below T_g, the nucleation rates could not reach their ultimate steady-state value because of premature crystallization.

Finally, we confirmed the stepwise increase of the nucleation rates, which we had discovered before for a single temperature, and interpreted such complex scenarios of glass dynamics as the result of stepwise structural relaxation using a new set of temperatures and times.

Our conclusion about the extremely long-term relaxation of the glass (as inferred by nucleation kinetics) is based on a thorough analysis of several nucleation experiments. Therefore, it would be stimulating to confirm it by direct structural methods. It should be emphasized that the nucleation rate is susceptible to changes in the state of the liquid since it affects both the kinetic and thermodynamic barriers. The current comprehensive study at temperatures well below T_g strongly indicates that the relaxation effect on crystal nucleation should be considered in any crystal nucleation model at deep supercoolings.

Acknowledgements

We are grateful to the São Paulo Research Foundation - FAPESP, project nos. 2013/007793-6 (CEPID) and 2022/00757-3, CAPES, project no. 88887.468838/2019-00, and CNPq, Brazil, for funding this research.

References

1. J. W. Gibbs. On the Equilibrium of Heterogeneous Substances. *Trans. Conn. Acad. Sci*. **3**, 108-248 (1875).
2. G. Tammann. *Der Glaszustand* ("The Glass State"). Leopold Voss Verlag, Leipzig, Germany (1933) 123 p.
3. R. Becker, W. Döring. Kinetische Behandlung der Keimbildung in übersättigten Dämpfen, *Ann. Phys*. **416**, 719-752 (1935). https://doi.org/10.1002/andp.19354160806
4. J. W. Christian, The Theory of Transformations in Metals and Alloys, Part I, Pergamon, Oxford (1981).
5. K. F. Kelton, A. L. Greer, Nucleation in condensed matter. Applications in Materials and Biology, Pergamon Mater. Series, vol. 15 (2010).
6. I. S. Gutzow, J. W. P. Schmelzer, The Vitreous State: Thermodynamics, Structure, Rheology, and Crystallization, First edition, Springer, Berlin, 1995; Second enlarged edition, Springer, Heidelberg, 2013.
7. V. M. Fokin, E. D. Zanotto, N. S. Yuritsyn, J. W. P. Schmelzer, Homogeneous Crystal Nucleation in Silicate Glasses: A Forty Years Perspective, J. Non-Crystalline Solids **352**, 2681–2714 (2006). https://doi.org/10.1016/j.jnoncrysol.2006.02.074
8. V. M. Fokin, A. M. Kalinina, V. N. Filipovich, Nucleation in silicate glasses and effect of preliminary heat treatment on it, J. Cryst. Growth **52**, 115–121 (1981). http://dx.doi.org/10.1016/0022-0248(81)90178-0
9. P. F. James, Kinetics of crystal nucleation in silicate glasses, J. Non-Cryst. Solids **73**, 517–540 (1985). http://dx.doi.org/10.1016/0022-3093(85)90372-2
10. R. S. Tiwari, Analysis of steady state crystal nucleation in metglas 2826, J. Non-Cryst. Solids **83**, 126–133 (1986). https://doi.org/10.1016/0022-3093(86)90062-1
11. A. S. Abyzov, V. M. Fokin, A. M. Rodrigues, E. D. Zanotto, J.W.P. Schmelzer, The effect of elastic stresses on the thermodynamic barrier for crystal nucleation, J. Non-Cryst. Solids **432**, 325–333 (2015). http://dx.doi.org/10.1016/j.jnoncrysol.2015.10.029
12. V. M. Fokin, A. S. Abyzov, E. D. Zanotto, D. R. Cassar, A. M. Rodrigues, J. W. P. Schmelzer, Crystal nucleation in glass-forming liquids: Variation of the size of the "structural units" with temperature, J. Non-Cryst. Solids **447**, 35–44 (2016). http://dx.doi.org/10.1016/j.jnoncrysol.2016.05.017
13. A. S. Abyzov, V. M. Fokin, N. S. Yuritsyn, A. M. Rodrigues, J. W. P. Schmelzer. The effect of heterogeneous structure of glass-forming liquids on crystal nucleation, J. Non-Cryst. Solids **462**, 32–40 (2017). https://doi.org/10.1016/j.jnoncrysol.2017.02.004

14. P. K. Gupta, D. R. Cassar, E. D. Zanotto, Role of dynamic heterogeneities in crystal nucleation kinetics in an oxide supercooled liquid, J. Chem. Phys. **145**, 211920/1–211920/8 (2016). http://dx.doi.org/10.1063/1.4964674

15. V. M. Fokin, A. S. Abyzov, N. S. Yuritsyn, J. W. P. Schmelzer, E.D. Zanotto, Effect of structural relaxation on crystal nucleation in glasses, Acta Mater. **203**, 116472 (2021). https://doi.org/10.1016/j.actamat.2020.11.014

16. J. W. P. Schmelzer, T. V. Tropin, V. M. Fokin, A. S. Abyzov, E. D. Zanotto: Effects of Glass Transition and Structural Relaxation on Crystal Nucleation: Theoretical Description and Model Analysis, Entropy **22**, 1098/1–36 (2020). doi:10.3390/e22101098

17. L. R. Rodrigues, A. S. Abyzov, V. M. Fokin, E. D. Zanotto, Effect of structural relaxation on crystal nucleation in a soda-lime-silica glass, J. Am. Ceram. Soc. **104**, 3212–3223 (2021). https://doi.org/10.1111/jace.17765

18. L. R. Rodrigues, A. S. Abyzov, V. M. Fokin, J. W. P. Schmelzer, E. D. Zanotto: Relaxation effect on crystal nucleation in a glass unveiled by experimental, numerical, and analytical approaches, Acta Materialia **223**, 117458/1–10 (2022). https://doi.org/10.1016/j.actamat.2021.117458

19. J. W. P. Schmelzer, T. V. Tropin: Theory of Crystal Nucleation of Glass-forming Liquids: Some New Developments, Int. J. Appl. Glass Sci. **13**, 171–198 (2022). https://doi.org/10.1111/ijag.16547

20. A. Morvan, L. Calvez, A. Vella, A. Saiter-Fourcin, Physical aging of the $62.5GeS_2$-$12.5Sb_2S_3$-25CsCl chalcogenide glass: Assessing the mechanisms of equilibration and crystallization, J. Non-Cryst. Solids **598** (2022) 121955. https://doi.org/10.1016/j.jnoncrysol.2022.121955

21. R. Androsch, C. Schick, J. W. P. Schmelzer, Sequence of enthalpy relaxation, homogeneous crystal nucleation and crystal growth in glassy polyamide 6, European Polymer Journal **53**, 100–108 (2014), https://doi.org/10.1016/j.eurpolymj.2014.01.012

22. R. Androsch, E. Zhuravlev, J. W. P. Schmelzer, C. Schick, Relaxation and crystal nucleation in polymer glasses, European Polymer Journal **102,** 195–208 (2018). https://doi.org/10.1016/j.eurpolymj.2018.03.026

23. A. Morvan, N. Delpouve, A. Vella, F. Saiter, Physical aging of selenium glass: Assessing the double mechanism of equilibration and the crystallization process, J. Non-Cryst. Solids **570**, 121013 (2021). https://doi.org/10.1016/j.jnoncrysol.2021.121013

24. C. Desgranges and J. Delhommelle, Unusual Crystallization Behavior Close to the Glass Transition, Phys. Rev. Lett. **120**, 115701 (2018) https://doi.org/10.1103/PhysRevLett.120.115701

25. C. Desgranges and J. Delhommelle, Non-monotonic variations of the nucleation free energy in a glass-forming ultra-soft particles fluid, Soft Matter, **14**, 5977-5985 (2018), https://doi.org/10.1039/C8SM00887F

26. G. Tammann, Über der Abhängigkeit der Zahl der Kerne, welche sich in verschiedenen unterkühlten Flüssigkeiten bilden, von der Temperatur (Engl: On the dependence of the number of nuclei, formed in an undercooled liquid, on temperature), Z. Phys. Chem. **25**, 441–479 (1898). https://doi.org/10.1515/zpch-1898-2526

27. R. T. DeHoff, Quantitative Microscopy, McGraw-Hill Book Company,1968.

28. A. S. Abyzov, J. W. P. Schmelzer, V. M. Fokin, E. D. Zanotto, Crystallization of Supercooled Liquids: Self-Consistency Correction of the Steady-State Nucleation Rate, Entropy **22**, 1–28 (2020), https://doi.org/10.3390/e22050558

29. D. R. Uhlmann, Crystal growth in glass forming systems: a ten years perspective. In Advances in ceramics, V4. Nucleation and crystallization in glasses. 1982. Edited by J. H. Simmons, D. R. Uhlmann & G. H. Beall. American Ceramic Society, Columbus, Ohio. Pp 80–124.

30. K. Takahashi, T. Yoshio, Thermodynamic quantities of alkali silicates in the temperature range from 25 °C to melting point, Yogyo-Kyokai-Sch **81**, 524–533 (1973).

31. M. L. F. Nascimento, V. M. Fokin, E. D. Zanotto, A. S. Abyzov, Dynamic processes in a silicate liquid from above melting to below the glass transition, J. Chem. Phys. **135**, 194703/1–18 (2011). https://doi.org/10.1063/1.3656696

32. D. Kashchiev, Solution of the non-steady state problem in nucleation kinetics, Surf. Sci. **14**, 209–220 (1969). https://doi.org/10.1016/0039-6028(69)90055-7

33. I. Gallino, D. Cangialosi, Z. Evenson, L. Schmitt, S. Hechler, M. Stolpe, B. Ruta, Hierarchical aging pathways and reversible fragile-to-strong transition upon annealing of a metallic glass former, Acta Materialia **144**, 400–410 (2018). https://doi.org/10.1016/j.actamat.2017.10.060

34. D. Cangialosi, V. M. Boucher, A. Alegría, J. Colmenero, Direct Evidence of Two Equilibration Mechanisms in Glassy Polymers, Phys. Rev. Let. **111**, 095701 (2013). https://doi.org/10.1103/PhysRevLett.111.095701

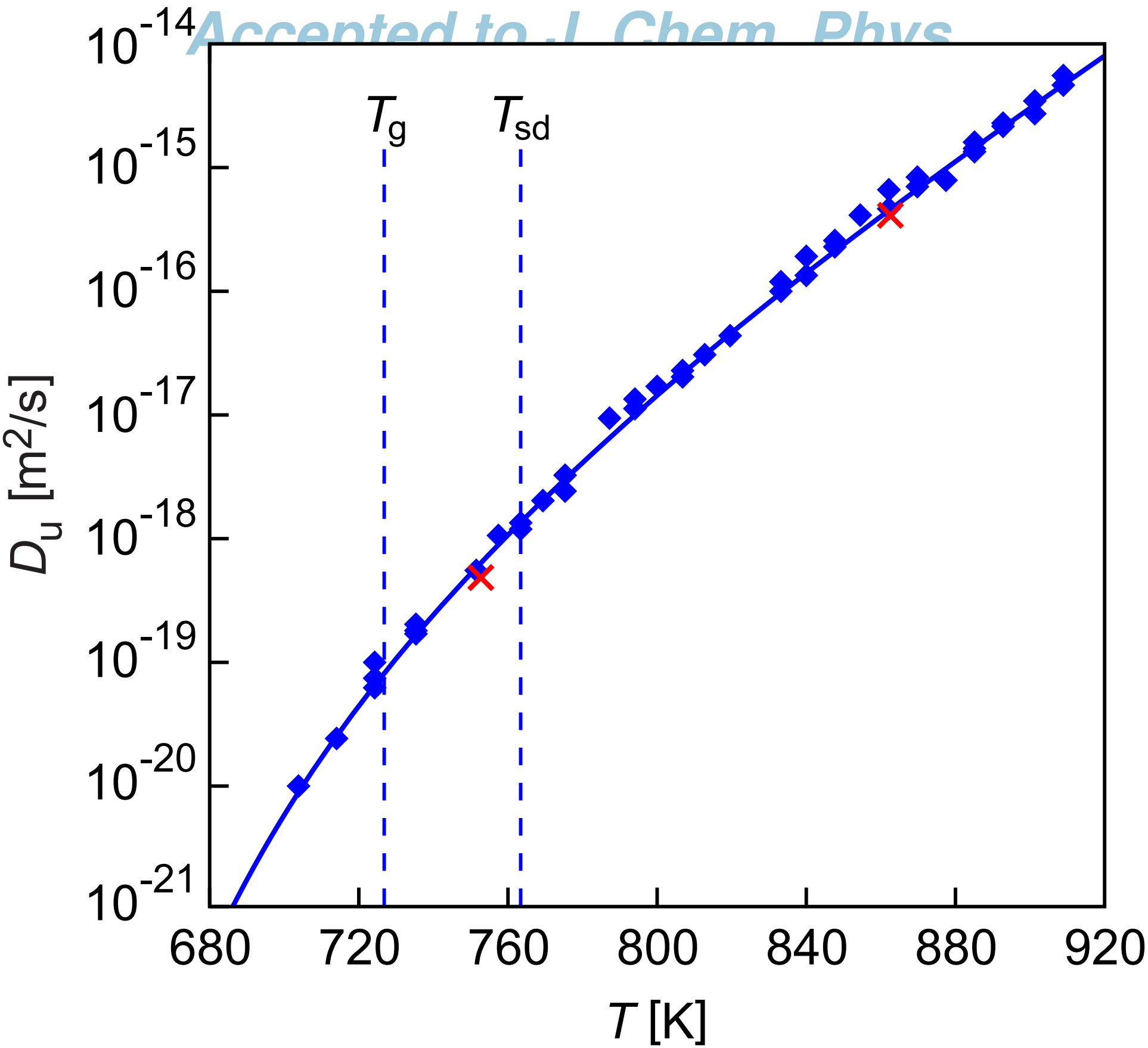

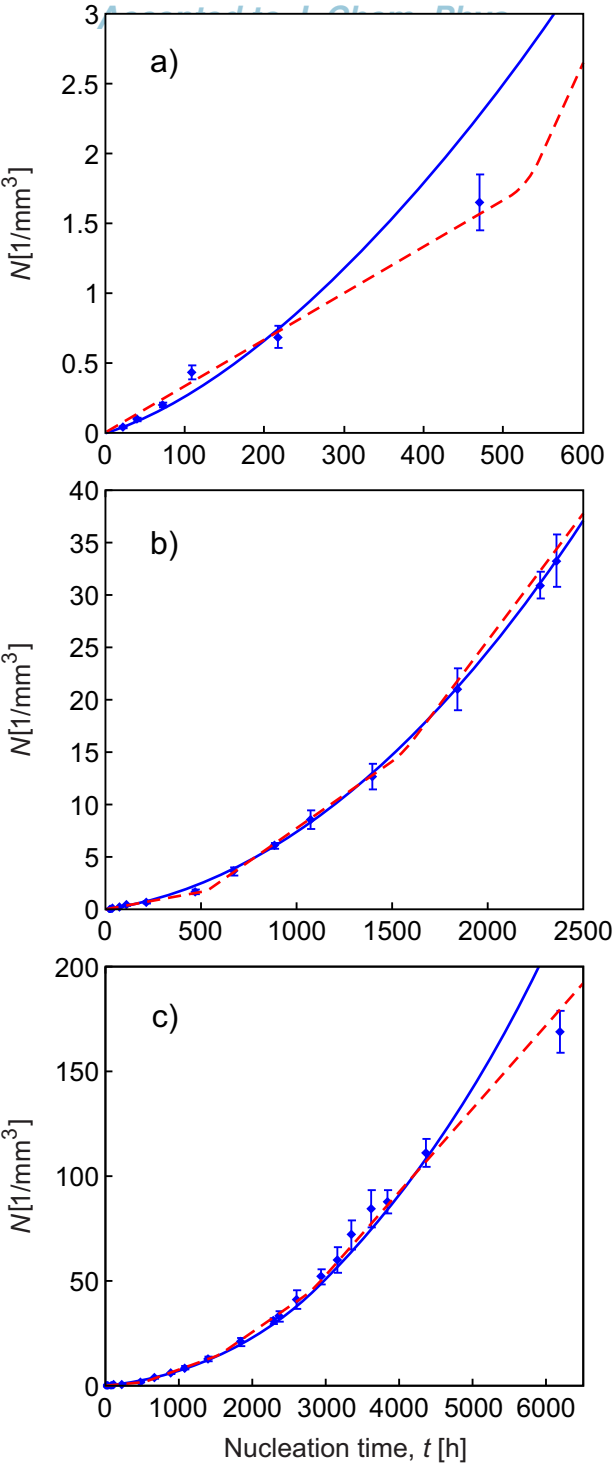

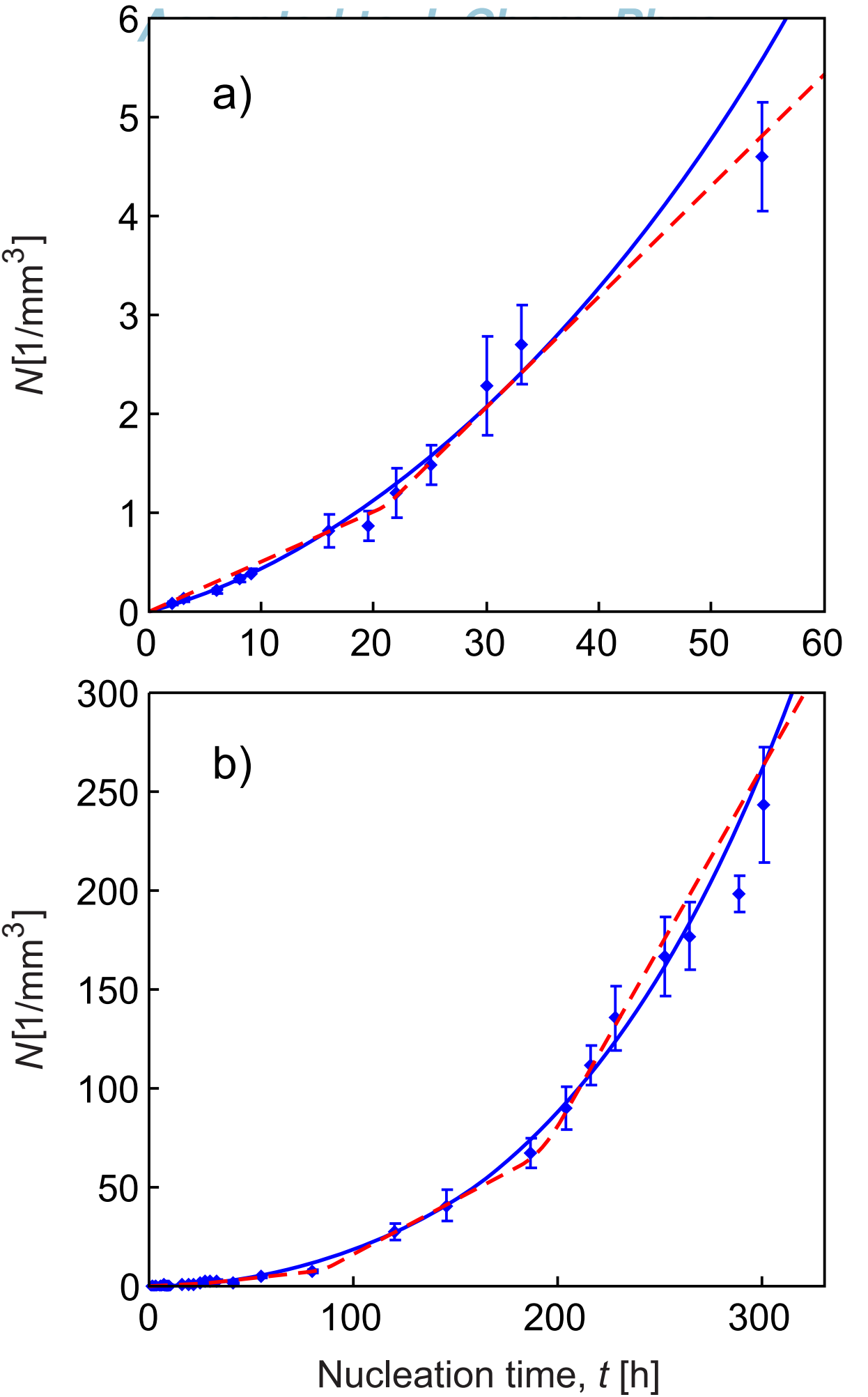
a)
b)
N[1/mm3]
N[1/mm3]
Nucleation time, t [h]
0
10
20
30
40
50
60
100
200
300
1
2
3
4
5
6
50
150
250

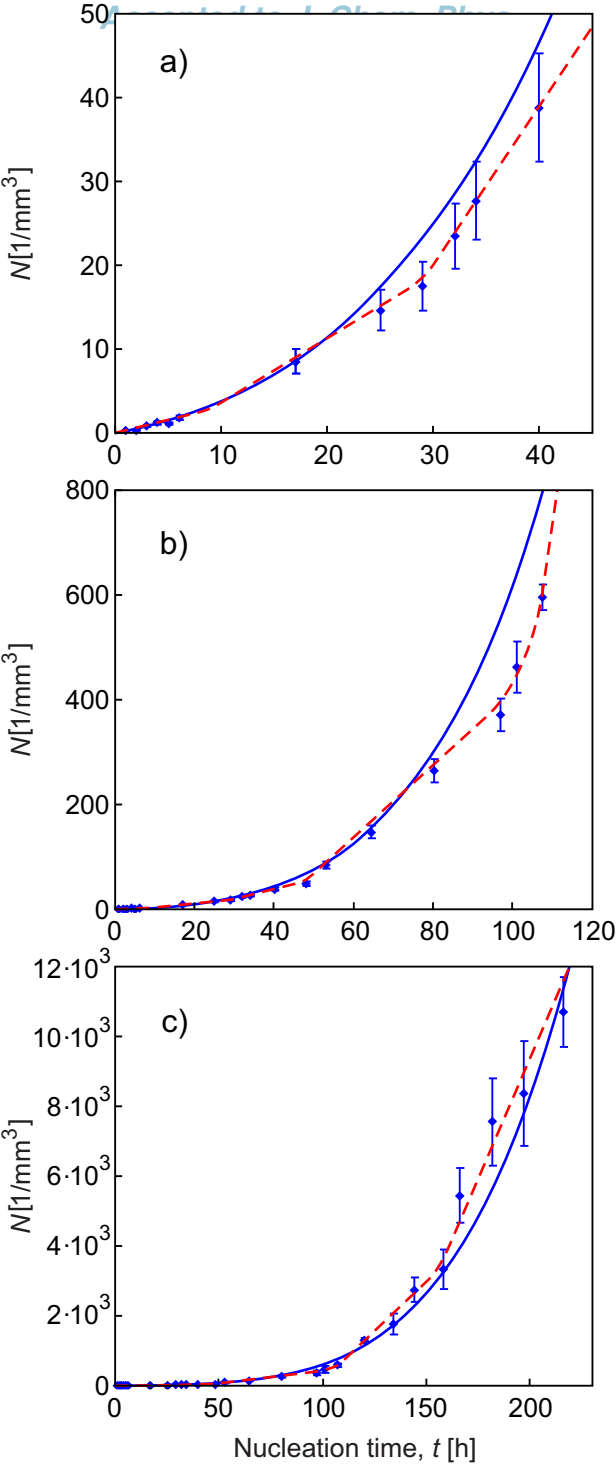
a)
b)
c)
N[1/mm3]
N[1/mm3]
N[1/mm3]
0
10
20
30
40
50
0
200
400
600
800
0
20
40
60
80
100
120
0
2·10^3
4·10^3
6·10^3
8·10^3
10·10^3
12·10^3
0
50
100
150
200
Nucleation time, t [h]

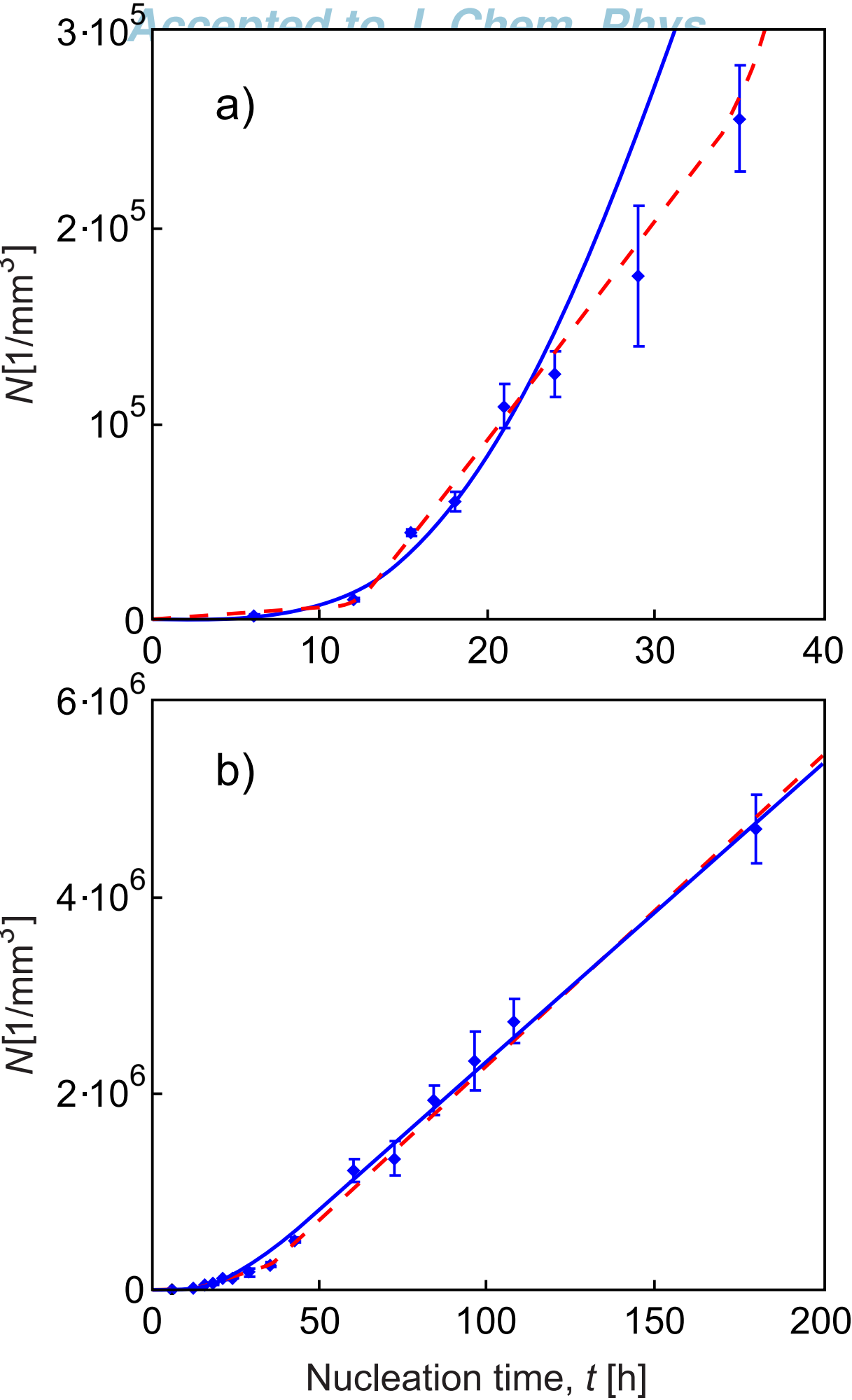

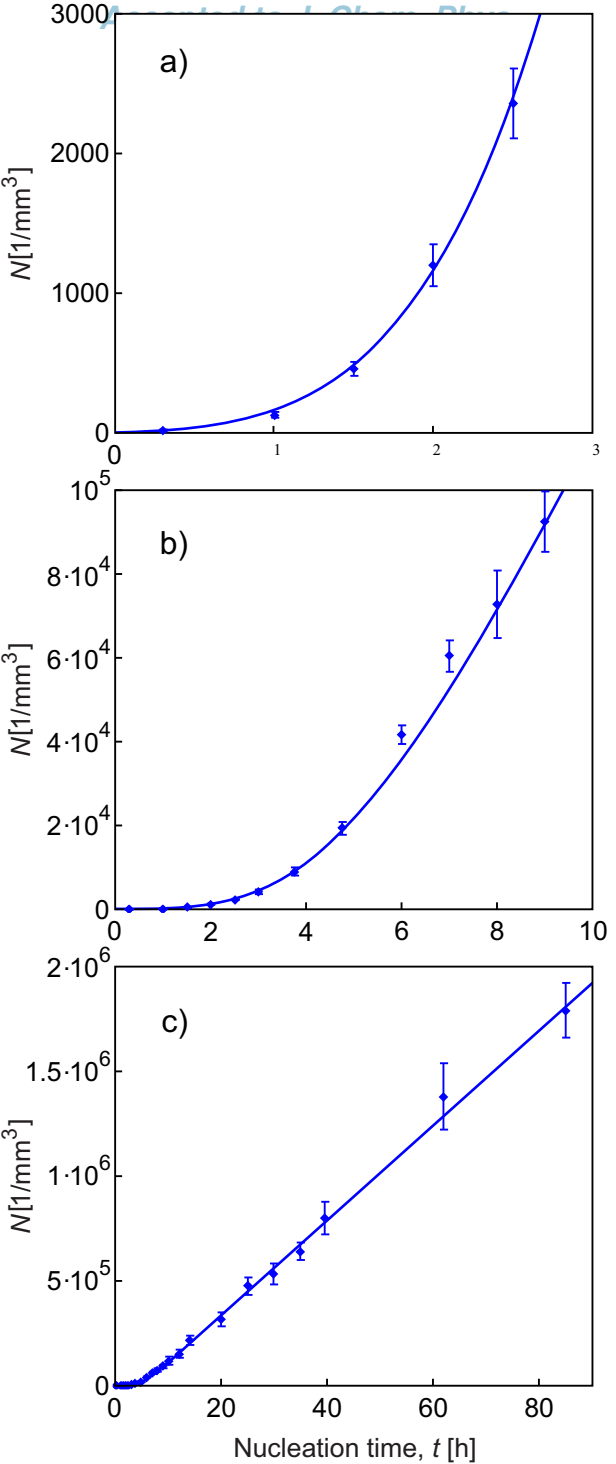
a)
b)
c)
N[1/mm3]
Nucleation time, t [h]

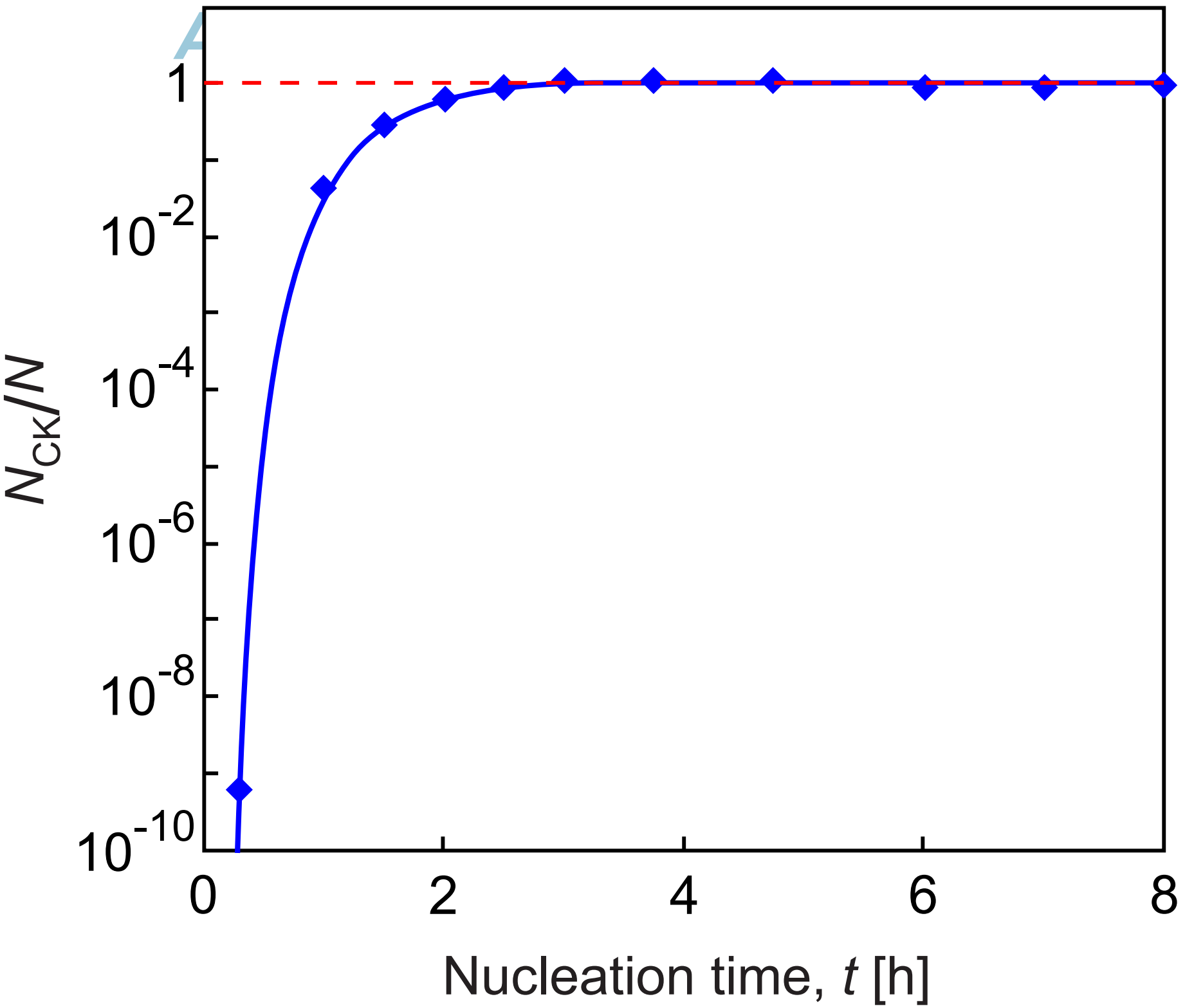
1
10^{-2}
10^{-4}
10^{-6}
10^{-8}
10^{-10}
N_{CK}/N
0
2
4
6
8
Nucleation time, t [h]

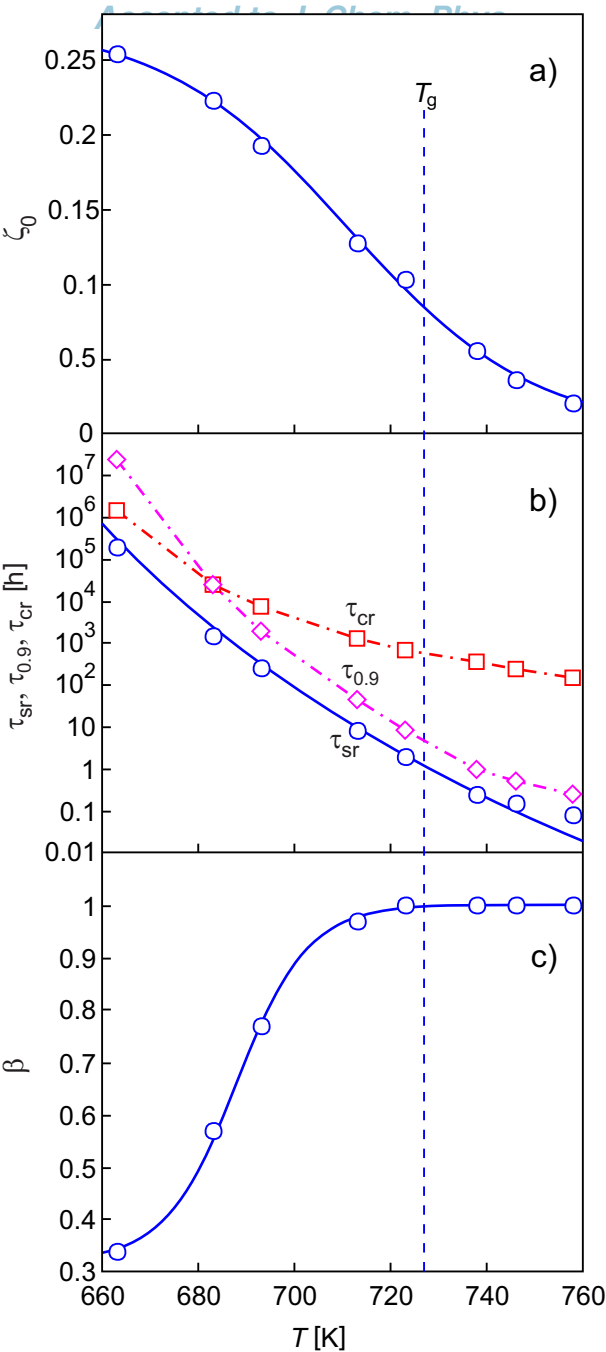
a)
b)
c)
T_g
ζ_0
τ_{sr}, $\tau_{0.9}$, τ_{cr} [h]
τ_{cr}
$\tau_{0.9}$
τ_{sr}
β
T [K]
0.25
0.2
0.15
0.1
0.5
0
10^7
10^6
10^5
10^4
10^3
10^2
10
1
0.1
0.01
1
0.9
0.8
0.7
0.6
0.5
0.4
0.3
660
680
700
720
740
760

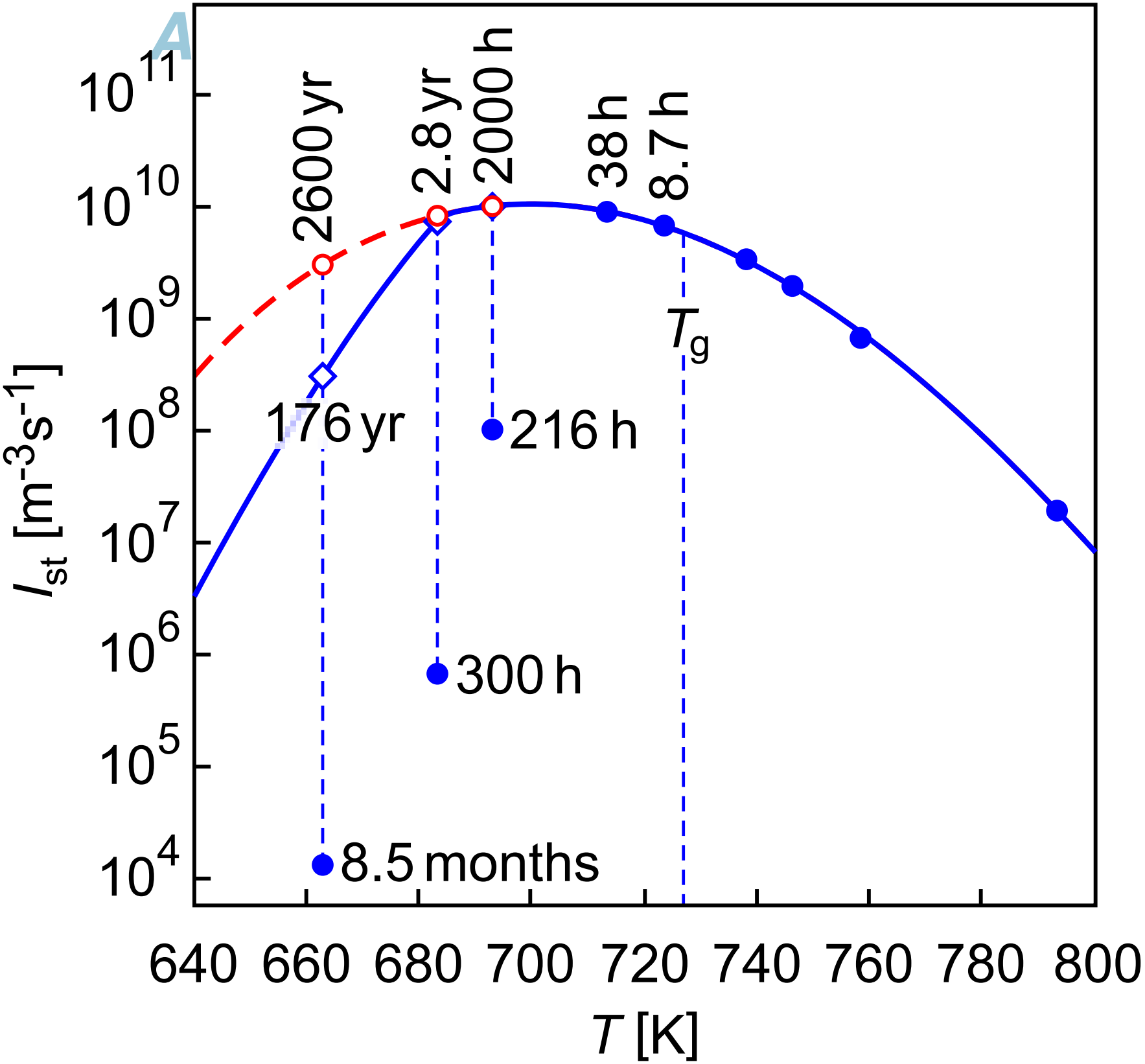
A
10^{11}
10^{10}
10^{9}
10^{8}
10^{7}
10^{6}
10^{5}
10^{4}
I_{st} [$m^{-3}s^{-1}$]
2600 yr
2.8 yr
2000 h
38 h
8.7 h
T_g
176 yr
216 h
300 h
8.5 months
640 660 680 700 720 740 760 780 800
T [K]